GEOLOGY AND HXRF GEOCHEMISTRY OF METAMORPHIC XENOLITHS IN TOWN MOUNTAIN GRANITE AT "THE SLAB" SWIMMING HOLE, LLANO UPLIFT, KINGSLAND, TEXAS

Liane M. Stevens*, Ethan Wagner, and Tyler McLemore
Department of Earth Sciences and Geologic Resources
Stephen F. Austin State University, Nacogdoches TX 75962
**Corresponding author; Email: stevenslm@sfasu.edu*

Abstract.–Metamorphic xenoliths in the Town Mountain Granite are exposed at "The Slab," a low-water crossing in Kingsland, Texas, that is popular both for recreation and as a stop on regional geology field trips to the Llano uplift. Difficulty in sampling the pavement-style outcrops limits observation and analysis to that which can be completed at the outcrop. We use structural orientation measurements and a handheld X-ray fluorescence spectrometer (hXRF) to study xenolith orientation in context of regional fabrics, assess evidence of xenolith assimilation into the Town Mountain Granite, and investigate the origin of the xenoliths based on bulk composition. A nearly 1:1 correlation between the orientations of the xenoliths' long axes and their internal foliation suggests that granite intrusion along foliation strongly controlled the xenoliths' shapes. The orientation of the xenoliths' foliation is consistent with dominant regional foliations. The hXRF analyses are able to discriminate between the compositions of the granite and the xenoliths. Xenolith compositions are consistent with a mafic protolith and suggest they have the same or similar sources; different analytical techniques for previously published bulk compositional analyses prevent direct comparison with our data or confident identification of a source unit. Limited assimilation of the xenoliths into the granite is suggested by magma injections into xenoliths, mafic residue from partial melting, chemical gradations at contacts between the granite and xenoliths, and possible enrichment of xenoliths in FeO + MgO relative to bulk compositions of the metamorphic country rock. These results encourage future use of hXRF for outcrop-based geological studies.

Keywords: assimilation, ACF diagram, bulk composition, gradational contact, nondestructive analysis.

The ~1.1 billion-year-old Town Mountain Granite that is exposed at "The Slab" swimming hole on the Llano River in Kingsland, Texas, a popular stop on regional geology field trips to the Llano uplift, is host to dozens of xenoliths of fine-grained, foliated metamorphic rock (Fig.

OPEN ACCESS DOI 10.32011/txjsci_75_1_Article3
Received: 24 June 2023 | Accepted: 23 Aug 2023 | Published Online: 12 Sept 2023

1). The xenoliths are presumably sourced from either the Valley Spring Gneiss (Valley Spring domain) or the Honey Formation (Packsaddle domain), both of which outcrop nearby. The xenoliths vary in size, shape, and orientation, and appear to exhibit a weak preferred orientation that may reflect the orientation of regional structural fabrics. Close inspection reveals variation in the style of contacts between the xenoliths and the Town Mountain Granite, which suggests varying degrees of xenolith assimilation into the intruding magma.

To address questions related to the xenoliths' origin, metamorphism, deformation, and intrusive processes, study should ideally include field work (textural descriptions, xenolith orientation, structural orientation), sample collection, thin section petrography, and bulk geochemical analysis. Unfortunately, responsible study of this site does not allow for sample collection nor for destructive analytical techniques because the smoothly scoured granite knobs at The Slab are popular among local residents for wading and playing, and because sampling the pavement-style outcrops is impractical (Fig. 1C).

The acquisition of a handheld X-ray fluorescence spectrometer (hXRF) by the Department of Earth Sciences and Geologic Resources at Stephen F. Austin State University makes it possible to study bulk chemical composition and chemical variation within both the xenoliths and the Town Mountain Granite, thereby reducing or eliminating much of the need to collect samples. Access to the hXRF enables field-based study of the xenoliths, with the goals of placing xenolith preferred orientation and xenolith schistosity within the context of the regional fabrics exposed within the Llano uplift; identifying evidence of xenolith assimilation into the Town Mountain Granite; and investigating the origin of the xenoliths based on bulk composition.

MATERIALS & METHODS

The study area is located at a popular swimming hole in Llano County, just north of Kingsland, Texas, called "The Slab" (Fig. 1B). The smooth, low, pavement-style outcrops are located in the bed of the

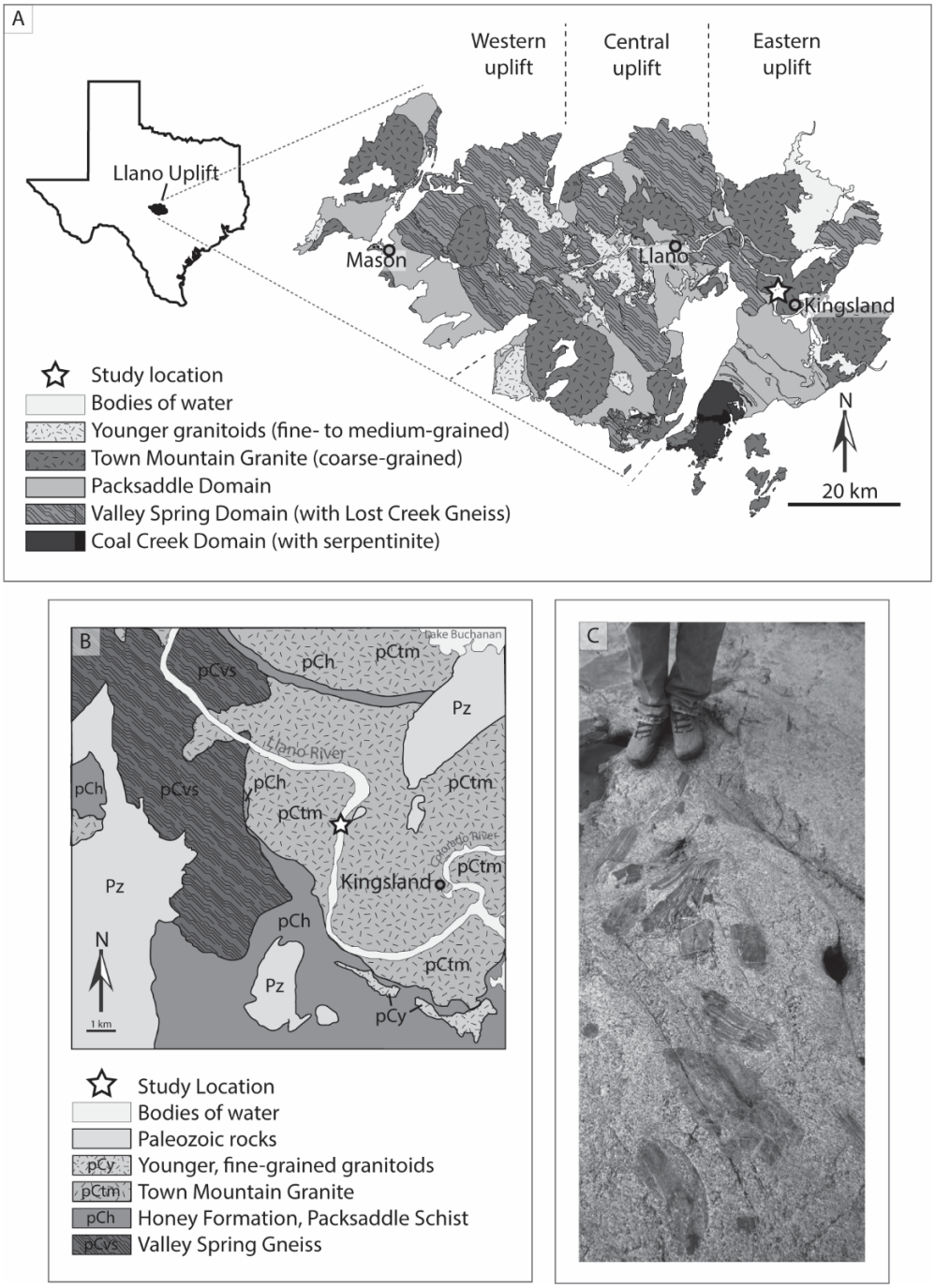

Figure 1. The location of the study area within the Llano uplift, Kingsland, Texas. A) A simplified lithotectonic map of the Llano uplift. The star marks the location of the study area. B) A geologic map of the study area (star) and surroundings. C) A photograph of a representative portion of the pavement-style outcrops in the study area showing the xenoliths (dark) within the Town Mountain Granite. Maps after USGS (2014) and Mosher et al. (2008).

Llano River, a navigable and, therefore, publicly accessible stream, just north of the low-water crossing on Slab Road/Ranch Road 3404 (30.685187, -98.482662). The outcrop is part of the Kingsland pluton of the Town Mountain Granite. The contact with the nearest country rock, which is mapped as the Honey Formation (Packsaddle domain) is approximately 2 km southwest of the study site (Fig. 1B), though the Valley Spring Gneiss also outcrops nearby (~3 km; USGS 2014).

The largest knobby granitic outcrop at the study site includes dozens of xenoliths, and was selected as the focus for study. For orientation measurements, a subset of 53 xenoliths was selected based on length (≥ 14 cm) and position. The number of xenoliths studied was limited by time constraints. Data collected for each xenolith include length (long axis;cm), width (short axis;cm), the trend and plunge of the long axis of the xenolith's exposed surface, the trend and plunge of the xenolith's foliation as it intersects with the outcrop's surface, and the strike and dip of the xenolith's foliation, if accessible. The aspect ratio for each xenolith was determined.

In lieu of sampling, a ThermoFisher Niton XL3 Handheld XRF Analyzer was used to measure elemental concentrations for points and along traverses from the granitic matrix into the fine-grained xenoliths (Fig. 2). The hXRF's "TestAll Geo" mode analyzes 45 major and trace elements (including metals and rare earth elements) between and inclusive of Mg (Z = 12) and U (Z = 92). Analyses had 3-8 mm spot sizes and a duration of 90-180 sec. Traverses crossed both sharp and gradational xenolith contacts.

To track the positions of hXRF analyses, removable multi-surface painter's tape was placed along the traverse and marked in 1 cm increments (Fig. 2A). The hXRF was placed alongside the tape, and a notch on the side of the device was aligned with the tic marks, which were numbered as analyses were collected (Fig. 2B). The hXRF snaps a photo of the greater analysis area (~1 cm diameter) at the start of an analysis, providing a visual check on the mineralogy and texture of the analyzed spot (Fig. 2C). For quality control, USGS/IAG standard

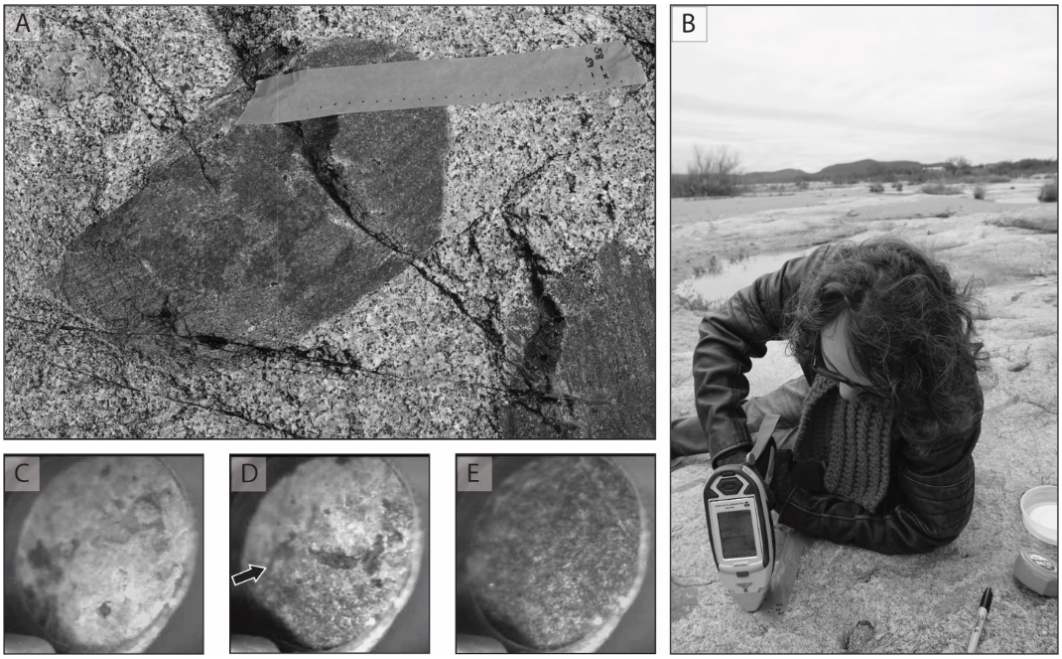

Figure 2. Methods for the use of the handheld XRF in the field. A) Painter's tape marked with 1 cm increments for a traverse across the sharp contact between the Town Mountain Granite and a xenolith. B) During use in the field, a notch on the side of the hXRF is aligned with the tic marks on the painter's tape. C) An image of the Town Mountain Granite captured by the hXRF at the start of an analysis. D) An image of the contact (arrow) between the Town Mountain Granite (top) and a xenolith (bottom) captured by the hXRF at the start of an analysis. E) A photo of a xenolith captured by the hXRF at the start of an analysis.

reference material SdAR-M2, a metal-rich sediment, was analyzed at the beginning and end of each run of analyses, as well as approximately once per hour, or roughly every 10 analyses (IAG 2015).

RESULTS

The xenoliths exposed at The Slab exhibit a variety of shapes, sizes, textures, and contact styles (Fig. 3). Xenoliths are fine-grained and dark in color with a slight greenish tinge. Most exhibit a gneissic foliation (Fig. 3A); it is possible that non-foliated xenoliths are actually foliated and exposed parallel to the foliation (Fig. 3B). The xenoliths tend to have relatively straight, sharp margins parallel to the internal foliation, though many exhibit gradational contacts, (Fig. 3A). Gradational

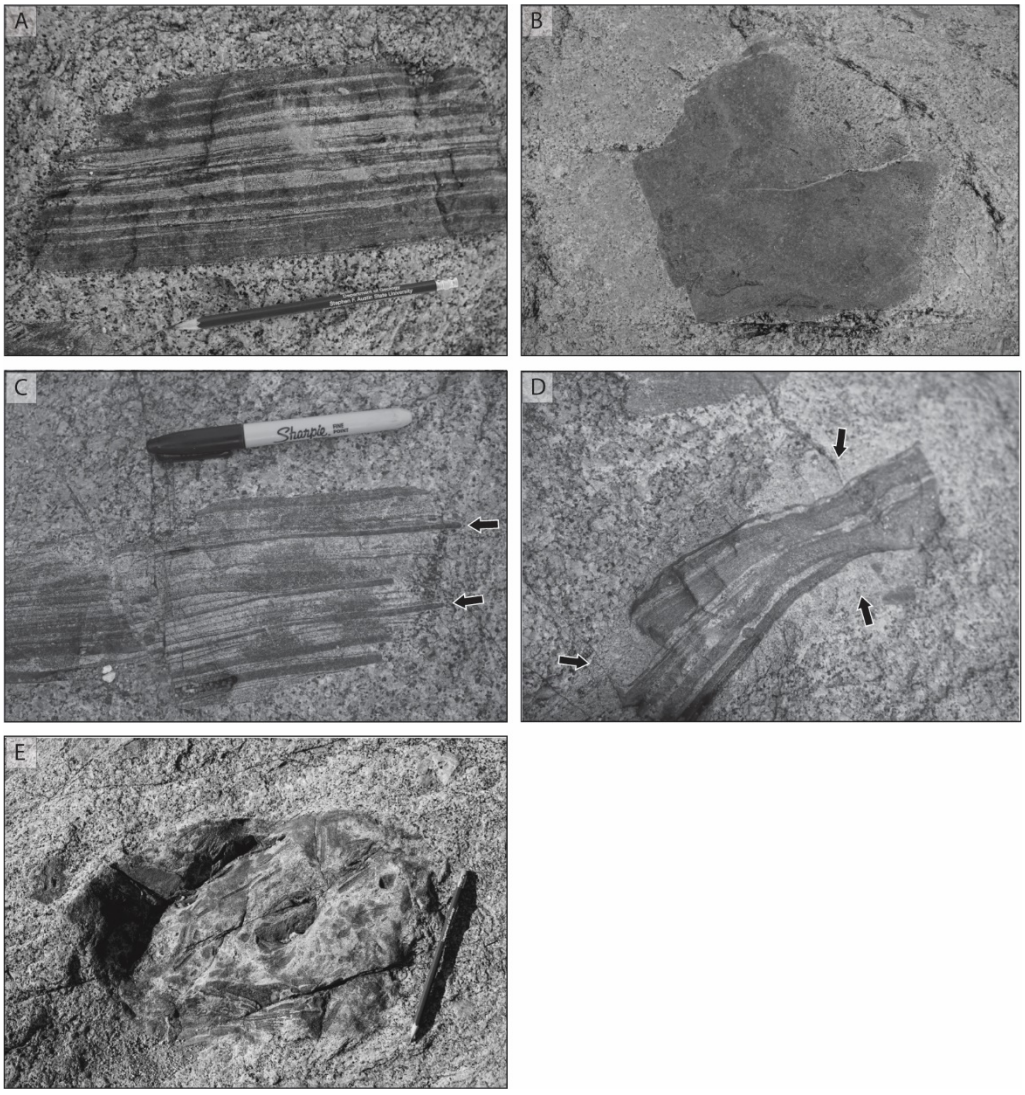

Figure 3. Photos of representative xenoliths in outcrops at the study area. A) A xenolith with a strong gneissic foliation, granitic "sills," and sharp contacts with the surrounding granite. B) A non-foliated xenolith with sharp contacts (left margin) and permeated gradational contacts (right margin). C) A foliated xenolith with permeated and injected gradational contacts. More mafic layers (arrows) persist into the surrounding Town Mountain Granite. D) A foliated xenolith with granite "sills" injected parallel to foliation. This xenolith is surrounded by a finer-grained granite (arrows) that may represent a chilled margin or more complex assimilation patterns. E) A patchy, non-foliated xenolith with permeated gradational contacts.

contacts were assessed visually based on variation in rock color, texture, or mineralogy. Small granitic "sills" run parallel to foliation (Fig. 3A, C, D). On some xenoliths, more mafic layers of foliation

persist into the granite matrix (Fig. 3C). A few xenoliths are immediately surrounded by a more fine-grained granite (Fig. 3D).

The xenoliths have an average length of 28.5 cm, ranging from 14.0-52.0 cm, and an average width of 13.3 cm, with a range of 3.5-36.0 cm. In general, longer xenoliths are likely to be wider. Aspect ratios (length/width) vary from 1 to 6.3, with an average aspect ratio of 2.6 (Fig. 4). Aspect ratios of 1.5-3.0 are most common. Xenoliths wider than 18.0 cm are confined to aspect ratios of 1-2; the narrowest xenoliths have the largest aspect ratios.

The orientation of each xenolith is represented by the trend and plunge of its long axis, as exposed on the outcrop surface; the plunge is indicative of the orientation of the outcrop surface rather than a representation of the true orientation of the xenolith in three dimensions. The xenoliths' long axes trend in a wide variety of directions, with a slight preference for ENE-WSW and ESE-WNW orientations (Fig. 4C).

The orientation of the foliation within the xenoliths is measured as the trend and plunge of the intersection lineation between the foliation and the outcrop's surface. These intersection lineations trend in a wide variety of directions, with slight preferences for ENE-WSW and SE-NW orientations (Fig. 4C). Foliation surfaces were exposed for only a few xenoliths. These surfaces strike ENE or WNW with moderate to steep dips. Most of the xenoliths show a 1:1 correlation between the trend of the long axis and the trend of the foliation intersection lineation (Fig. 4B).

Oxide concentration (wt%) varies among analyses of granite and among analyses of xenoliths. Granite analyses were expected to vary more greatly due to granite's coarser grain size and mineralogical variety, though this is not necessarily the case. Despite the variation, oxide concentration along traverses changes distinctly across contacts from the granite into the xenoliths (Figs. 5-6).

The xenoliths typically have lower SiO_2 concentrations and greater Al_2O_3,FeO, and MgO than the granite (Figs. 7-8). For the granite, values range from 0.18-6.91 wt% FeO, 6.94-31.43 for wt% Al_2O_3, 55.56-86.38 wt% SiO_2, and 0.00-1.46 wt% MgO. For the xenoliths, values range from 1.02-8.45 wt% FeO, 17.45-40.16 wt% Al_2O_3, 41.24-

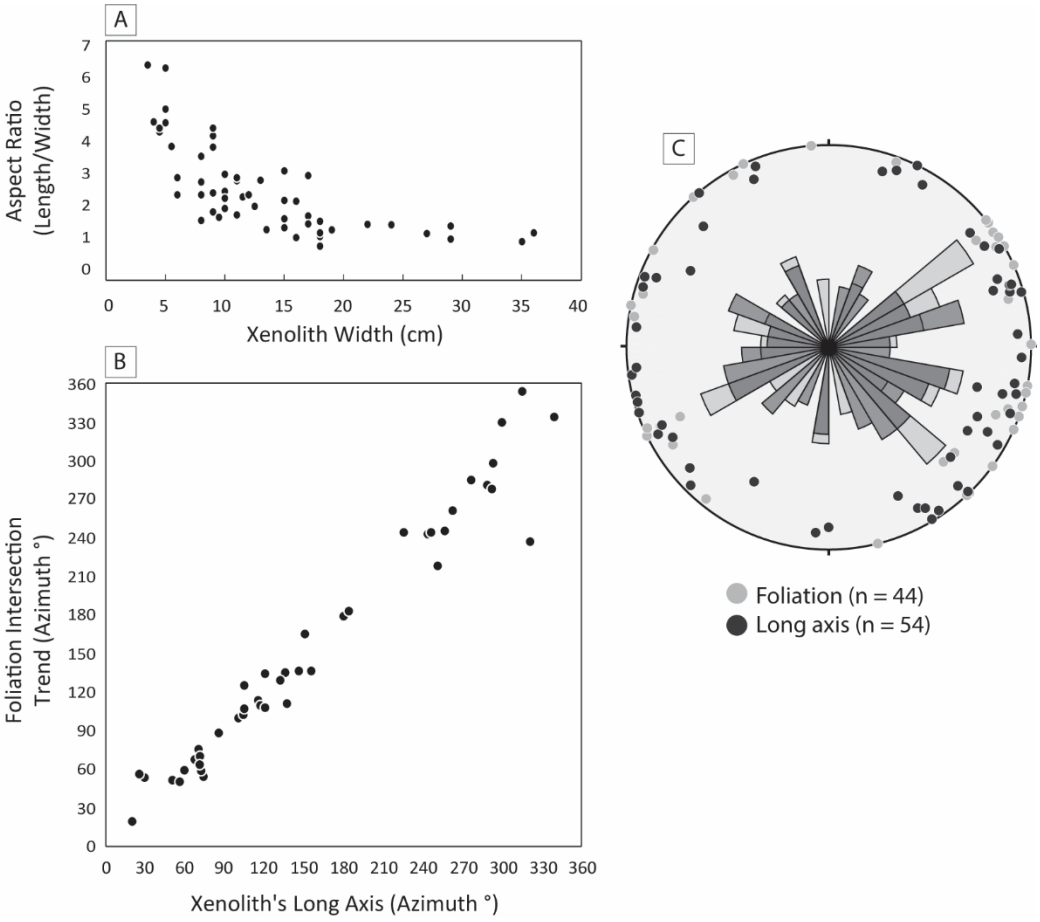

Figure 4. Measurements of xenolith size, aspect ratio, and orientation. A) The aspect ratio of the xenolith plotted versus its width shows that aspect ratios tend to be low, and that the most elongate xenoliths (highest aspect ratios) tend to be relatively narrow. B) The trend of the intersection lineation between the xenoliths' foliation and the outcrop surface plotted against the trend of the xenoliths' long axes shows a roughly 1:1 correlation. C) A lower hemisphere stereonet and a rose diagram showing trend and plunge for the foliation's intersection lineation and for the xenoliths' long axes. The diagram was plotted using Stereonet v. 11 (Allmendinger et al. 2011; Cardozo & Allmendinger 2013).

85.71 wt% SiO_2, and 0.00-2.79wt% MgO. There is greater overlap in concentration values of CaO and K_2O between the granite and the xenoliths, though the highest values for K_2O tend to be in the xenoliths. Analyses with 0.00 wt% MgO may simply have fallen below the instrument's level of detection for Mg.

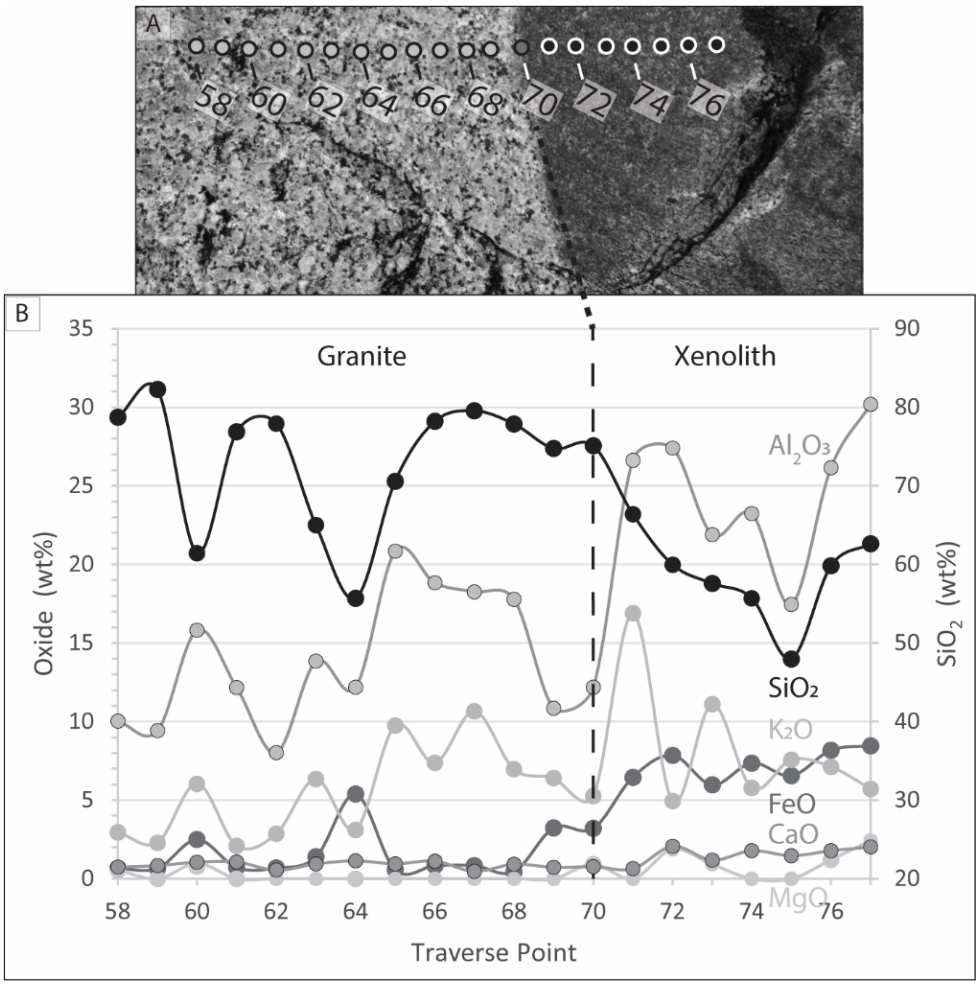

Figure 5. An hXRF traverse across a sharp contact between the granite and a xenolith. A) A photo of the area of the traverse with the locations of hXRF analyses marked. Analyses are equally spaced at ~1 cm intervals. B) A scatter plot showing the variation in the concentrations of SiO_2, Al_2O_3, K_2O, FeO, CaO, and MgO along the traverse. The plot is roughly aligned with the photo; the dashed line represents the location of the contact between the granite and the xenolith along the traverse.

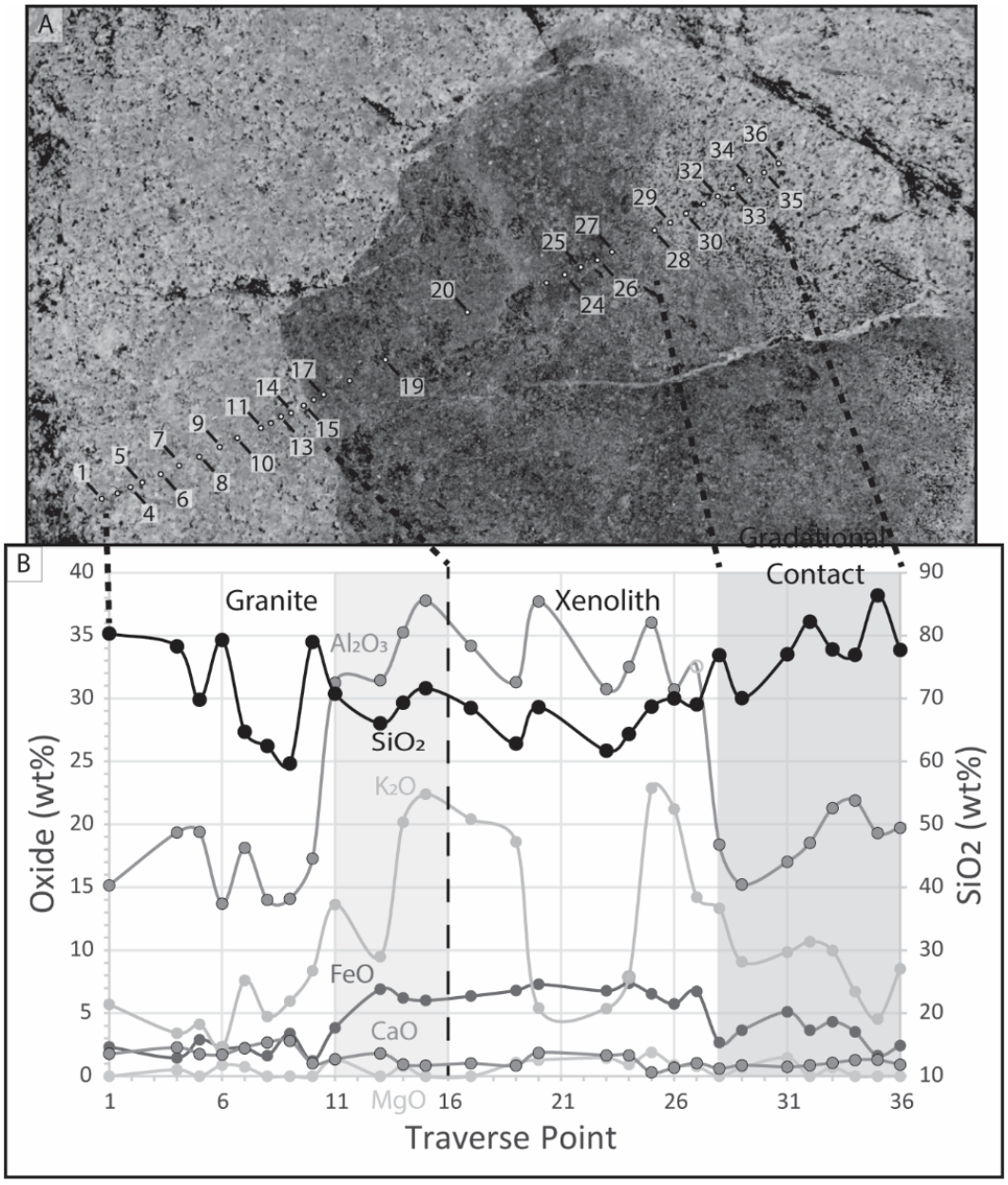

Figure 6. An hXRF traverse across a xenolith that includes a sharp contact on one side and a gradational contact on the other side. A) A photo of the area of the traverse with the locations of the hXRF analyses marked. Analyses across the granite and the gradational contact are approximately equally spaced (~1 cm); the analyses across the center of the traverse are not equally spaced. The dashed lines correlate points along the traverse with the points on the scatter plot. B) A scatter plot showing the variation in the concentrations of SiO_2, $Al2O_3$, K_2O, FeO, CaO, and MgO along the traverse. The dashed line represents the location of the sharp contact between the granite and the xenolith. The shaded areas represent analyses with transitional oxide concentrations, thought to represent gradational contacts.

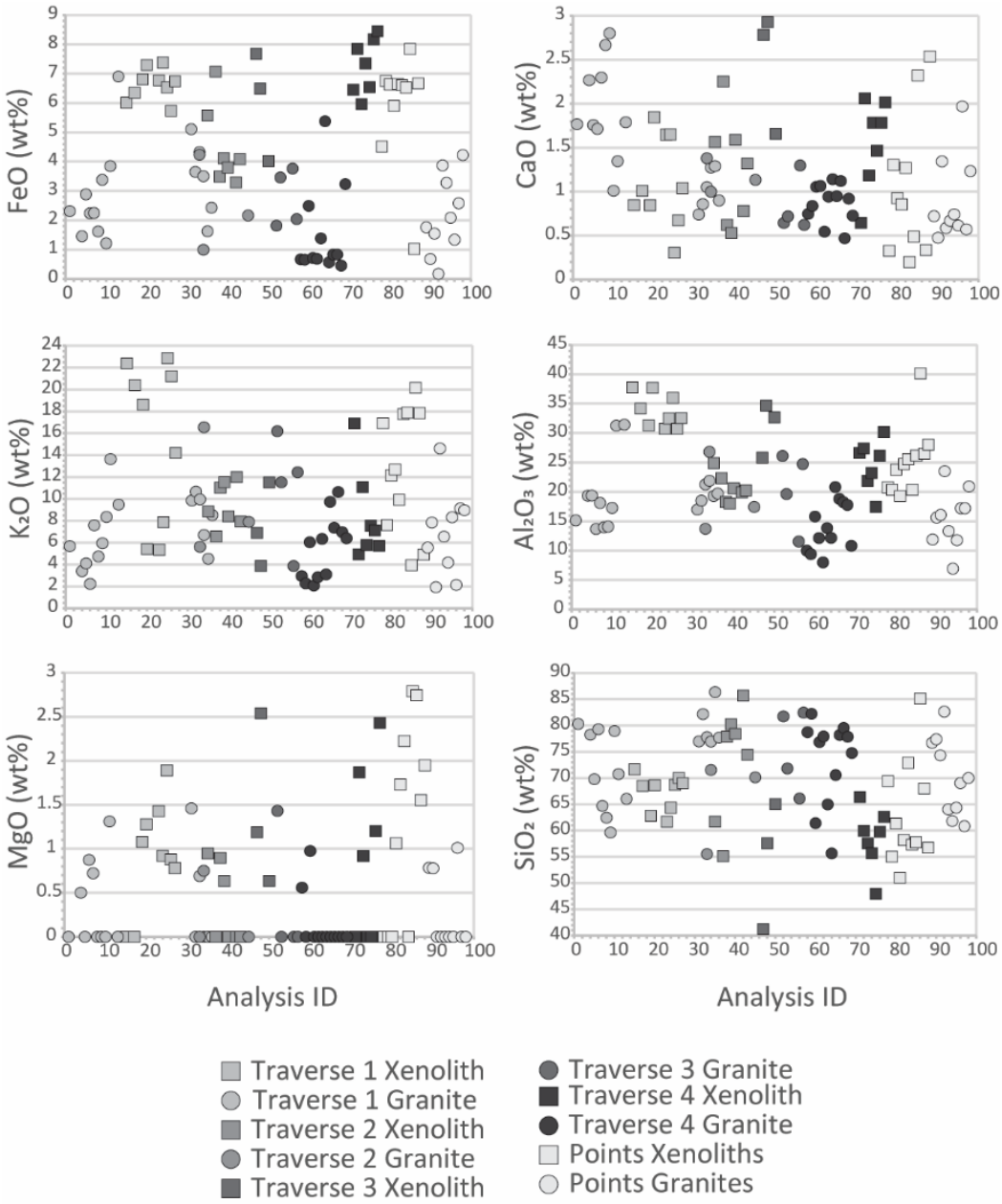

Figure 7. Oxide concentrations (wt%) of FeO, CaO, K_2O, Al_2O_3, MgO, and SiO_2 for all granite (circles) and xenolith (squares) analyses.

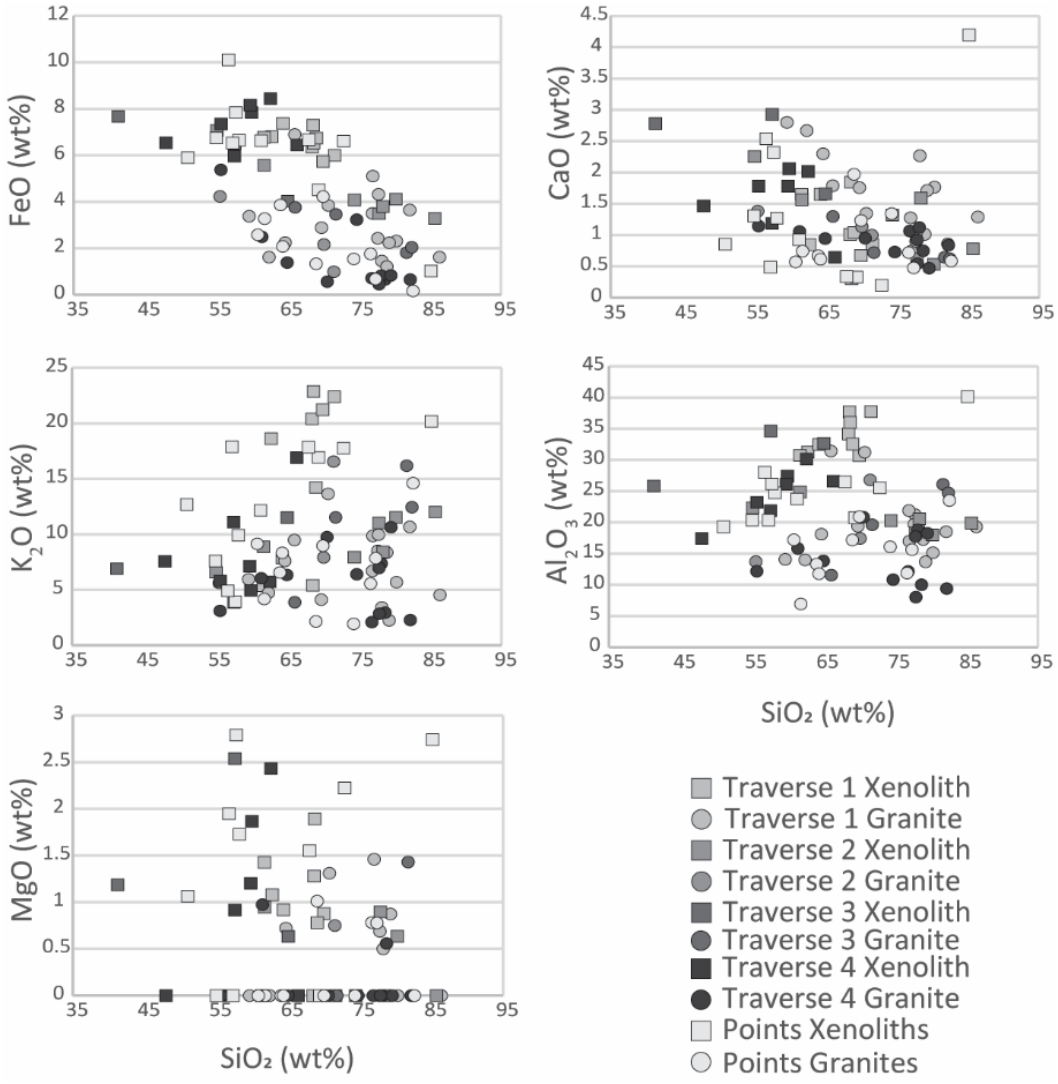

Figure 8. Harker variation diagrams for FeO, CaO, K_2O, Al_2O_3, and MgO (wt%) for all analyses of the granite (circles) and the xenoliths (squares).

DISCUSSION

Textures at the margins of the xenoliths are suggestive of interaction between the Town Mountain Granite and the country rock. Gradational contact styles include possible injected contacts and permeated contacts. In some cases, granitic melt appears to have been injected parallel to the xenoliths' foliation, though other apparent "sills" are

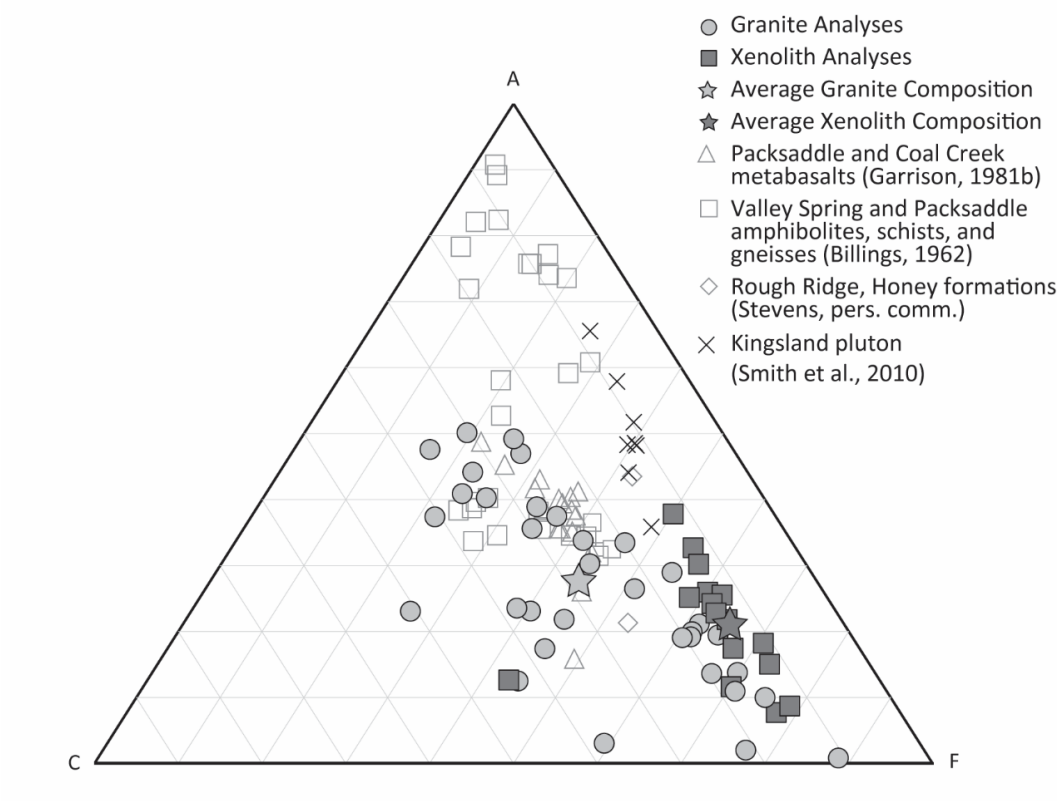

Figure 9. Granite and xenolith hXRF analyses plotted on an ACF diagram. All granite (filled circles) and xenolith (filled squares) analyses from Traverse 1, Traverse 4, and individually collected points are plotted. The average granite and xenolith compositions were calculated and plotted as stars. Bulk compositional data from the Kingsland Granite (X symbols; Smith et al., 2010) and from the Packsaddle and Valley Spring domains are plotted for comparison (unfilled symbols; Billings 1962; Garrison 1981; Stevens pers. comm.). A = Al_2O_3 - K_2O; C = CaO; F = FeO + MgO + MnO.

bordered by mafic minerals, which is consistent with the mafic selvage found adjacent to leucosome in a migmatite. Thus, some of these granitic layers are likely a product of metamorphism prior to the intrusion of the Town Mountain Granite. These layers are too thin to allow for hXRF analysis to compare with the bulk geochemistry of the Town Mountain Granite.

The permeated gradational contacts are characterized by smooth variation in color and mineralogy between the xenolith and the granite (Fig. 3B) and/or the persistence of mafic layers from xenoliths into the

granite (Fig. 3C) These textures are consistent with assimilation of the xenolith through partial melting and/or disaggregation, as mafic minerals or layers may persist as a residue because of their more refractory compositions. Assimilation is expected to be limited because the energy required to melt the xenoliths is too great and the process is self-limiting (e.g., Glazner 2007). This is consistent with the large numbers and relatively small sizes of the xenoliths.

The xenoliths vary in shape, size, and structural orientation. The correlation between the trend of the long axis of each xenolith and the trend of its foliation suggests that xenolith shape is strongly controlled by foliation. The scatter of foliation orientation is interpreted to represent the pre-intrusion polydeformational history of the country rock (Nelis et al. 1989; Mosher et al. 2004; Levine & Mosher 2010), as well as reorientation of xenoliths during intrusion. Four of the five foliations that have been identified in the uplift (S_1-S_3, S_5) trend NW-SE; only S_4 trends NE-SW. The SE-NW trend of the xenoliths' foliation is consistent with the dominant foliations (S_1, S_2) in the uplift. The slightly greater prevalence of ENE-WSW xenolith foliations may be consistent with the orientation of S_4.

While there is variation among analyses of the same rock type, the hXRF successfully discriminates between granite and the xenoliths on the basis of wt% FeO, wt% Al_2O_3, wt% SiO_2 and wt% MgO, with some overlap (Figs. 7, 8). This is seen both in comparisons of individual analyses and along traverses. For a traverse across a visually sharp contact between granite and a xenolith , upon entering the xenolith the concentration of SiO_2 decreases, while the concentrations of Al_2O_3, FeO, and CaO increase; the highest values for K_2O and MgO concentrations are in analyses of the xenolith. In another traverse (Fig. 6), the traverse enters a xenolith at a visually sharp contact and exits the xenolith at a gradational contact. Within the xenolith, SiO_2 concentration is consistently low compared to the granite, while Al_2O_3 and FeO concentrations are elevated. Elevated K_2O concentrations are seen at both xenolith margins. At the gradational contact, the element concentrations vary gradually. Unexpectedly, the elemental concentration variation at the visually sharp margin is similar to the gradual variation across the gradational contact. The gradual variation

in chemistry at this “sharp” contact may represent granite assimilation, diffusion, or the influence of unseen, subsurface xenolith material, particularly because this xenolith is likely exposed parallel to its foliation.

Harker variation diagrams (Fig. 8) are useful for comparing the range of compositions between the granite and xenolith analyses, although they are traditionally used to assess compositional trends in suites of igneous rocks in which bulk composition varies due to processes related to magma genesis and differentiation. The wide spread in SiO_2 values among granite analyses in this study is most likely due to compositional subsampling that results when analyzing a coarse-grained sample. Variation might also be expected if there has been some xenolith assimilation into the granite, though a relatively felsic partial melt would be expected to have limited influence. The Harker diagrams show that, in general, the xenoliths have greater Al_2O_3, K_2O, FeO, and MgO. Xenolith compositions are most easily distinguished from the granite in the Harker diagrams for FeO and Al_2O_3.

When bulk compositional analyses are plotted on a standard ACF diagram, the xenoliths plot primarily in the region near the F corner (FeO + MgO + MnO), which is where metamorphic rocks with mafic protoliths are expected to plot (Fig. 9). The relatively tight cluster of xenolith analyses suggests that the xenoliths do originate from the same or similar crustal source(s). The granite analyses plot near the center of the diagram, consistent with rocks of quartzofeldspathic compositions. A number of granite analyses plot near the xenolith analyses, but are slightly more Ca-enriched. These points are associated with analyses located within gradational contacts or analyses that captured an area of the rock dominated by mafic minerals.

Bulk compositional analyses from the Kingsland pluton are plotted on Fig. 9 for comparison with the granite analyses (Smith et al. 2010). The Kingsland pluton analyses are similar to the granite analyses in terms of the A and F components, but are lower in the C component than the granites from The Slab. The two analyses from fine-grained Kingsland pluton samples plot closest to the A corner, and are least similar to granite analyses from this study. The variation between the

two sets of samples may derive from different analytical procedures (the Kingsland pluton samples were analyzed using traditional XRF methods), differences in sample lithologies, and/or enrichment of CaO in the hXRF analyses, perhaps through the oversampling of plagioclase.

One of the goals of this work was to identify the bedrock source of the xenoliths in the study area, which we expected to do through comparison with previously published bulk compositional analyses. There are few such studies, so our comparisons are limited to data from Billings (1962), Garrison (1981), and two data points from Stevens (pers. comm.). Billings (1962) used bulk compositional data to identify the protoliths of the Packsaddle schist as mafic tuffs and tholeiitic basalts, and protoliths of the Valley Spring gneiss as granitoids or arkosic sediments. Garrison (1981) studied the geochemistry of Packsaddle and Coal Creek metabasalts and metagabbros. Standard XRF analyses were performed for one sample each of the Honey and Rough Ridge formations of the Packsaddle domain (Stevens pers. comm.).

The older datasets overlap the granite analyses from this study on the ACF diagram (Fig. 9). While this makes sense for samples of the Valley Spring gneiss analyzed by Billings (1962), it doesn't identify a source for the xenoliths in the study area. Further, several of Billings' (1962) samples plot much nearer the A corner ($Al_2O_3 + Fe_2O_3 - K_2O - Na_2O$), which is likely due to the influence of Fe_2O_3, which is accounted for in Garrison's and Billings' data, but not in the rest of the data. Further comparison of these data sets is likely unreliable due to the use of different analytical methods (hXRF vs. spectrophotometry and colorimetry). While the XRF bulk geochemistry of the Rough Ridge and Honey formations aligns most closely to the composition of the xenoliths, it is not sufficient for a positive identification.

The xenolith compositions vary in both A and F components (Fig. 9), which could be consistent with varying degrees of partial melting, assuming this causes enrichment of FeO + MgO and depletion of Al_2O_3 in the residual xenoliths. If so, this partial melting would shift the position of xenolith analyses towards the F corner of the ACF diagram. This could explain the offset of the xenolith analyses from the bulk

compositions for the Rough Ridge and Honey Creek samples, the Packsaddle and Coal Creek metabasalts, and amphibolites and schists from the Valley Spring and Packsaddle domains (Billings, 1962; Garrison, 1981b; Stevens, pers. comm.). Thus, despite the inability to positively identify a source lithology, none of these potential source rocks can be ruled out yet.

The xenoliths at The Slab are an interesting landmark to explore with students while touring the geology of the Llano uplift. Students can observe rock types, compositional and textural variations, interaction between country rock and intruding granite, structural fabrics and orientations, as well as more recent fractures, offset, differential weathering, and a number of surface processes. The shape of these xenoliths is strongly controlled by pre-existing foliation, and it is likely that the xenoliths show at least a weak to moderate preferred orientation consistent with some of the dominant regional fabrics. Permeated gradational contacts and other textures are consistent with limited assimilation of the xenoliths by the granite.

This data from the first field test of our new hXRF on crystalline rocks is used to evaluate the degree of xenolith assimilation and the usefulness of this tool on a typical regional outcrop where geologic sampling is not acceptable. Outcrop-based hXRF analyses are able to discriminate between the Town Mountain Granite and xenolith compositions, and contacts are clearly identified. Gradational contacts exhibit gradational bulk geochemistry, as does the granite at some “sharp” contacts, which suggests assimilation, chemical diffusion, or other influences on granite geochemistry that were not originally predicted by observation of the contacts.

The use of field-based handheld XRF spectrometry has been deployed in disciplines where access to samples must be automated or where nondestructive methods are essential, such as the use of micro-XRF instrumentation on the Mars rovers or identification of artifact source rocks in archeology, but has not been common in the land-based geosciences (e.g., Young et al. 2016; Allwood et al. 2020; Tibbits et al. 2022). This study demonstrates that the use of hXRF and the methods employed here are effective for determining differences in bulk rock

composition and detecting general compositional trends in the field, even for coarse-grained rocks.

The use of the hXRF is limited by spot size, element range, rock texture, and outcrop surface topography. Future work on this project will include study of trace elements from the hXRF analyses in this study, bulk geochemical analysis for an array of samples from the Packsaddle and Valley Spring domains, and more detailed analysis of the opportunities and limitations of the use of the hXRF on crystalline rocks for geologic studies.

ACKNOWLEDGMENTS

We thank former SFA undergraduate students Tyler West and Luke Whitenburg for their assistance in the field, Dr. Julie Bloxson for training and assistance with the hXRF, and the Department of Earth Sciences and Geologic Resources at Stephen F. Austin State University for support for this project. We also thank two anonymous reviewers for their constructive reviews. Liane Stevens provided unpublished bulk compositional XRF data for the Rough Ridge and Honey formations.

LITERATURE CITED

Allmendinger, R.W., N. Cardozo & D. Fisher. 2011. Structural geology algorithms: Vectors and tensors. Cambridge Univ. Press, Cambridge, 302 pp.

Allwood, A. C., Wade, L. A., Foote, M. C., Elam, W. T., Hurowitz, J. A., Battel, S., Dawson, D. E., Denise, R. W., Ek, E. M., Gilbert, M. S., King, M. E., Liebe, C. C., Parker, T., Pedersen, D. A. K., Randall, D. P., Sharrow, R. F., Sondheim, M. E., Allen, G., Arnett, K., Au, M. H., Basset, C., Benn, M., Bousman, J. C., Braun, D., Calvet, R. J., Clark, B., Cinquini, L., Conaby, S., Conley, H. A., Davidoff, S., Delaney, J., Denver, T., Diaz, E., Doran, G. B., Ervin, J., Evans, M., Flannery, D. O., Gao, N., Gross, J., Grotzinger, J., Hannah, B., Harris, J. T., Harris, C. M., He, Y., Heirwegh, C. M., Hernandez, C., Hertzberg, E., Hodyss, R. P., Holden, J. R., Hummel, C., Jadusingh, M. A., Jorgensen, J. L., Kawamura, J. H., Kitiyakara, A., Kozaczek, K., Lambert, J. L., Lawson, P. R., Liu, Y., Luchik, T. S., Macneal, K. M., Madsen, S. N., McLennan, S. M., McNally, P., Meras, P. L., Muller, R. E., Napoli, J., Naylor, B. J., Nemere, P., Ponomarev, I., Perez, R. M., Pootrakul, N., Romero, R. A., Rosas, R., Sachs, J., Schaefer, R. T., Schein, M. E., Setterfield, T. P., Singh, V., Song, E., Soria, M. M.,

Stek, P. C., Tallarida, N. R., Thompson, D. R., Tice, M. M., Timmermann, L., Torossian, V., Treiman, A., Tsai, S., Uckert, K., Villalvazo, J., Wang, M., Wilson, D. W., Worel, S. C., Zamani, P., Zappe, M., Zhong, F. & R. Zimmerman. 2020. PIXL: Planetary Instrument for X-Ray Lithochemistry. Space Sci Rev. 216(134):1-132.

Billings, G. K. 1962. A Geochemical Investigation of the Valley Spring gneiss and Packsaddle schist, Llano Uplift, Texas. Unpublished M.S. thesis, Rice Univ., Houston, 40 pp.

Cardozo, N. & R. W. Allmendinger. 2013. Spherical projections with OSXStereonet: Comput. Geosci. (51):193-205.

Garrison, J. R., Jr. 1981. Metabasalts and metagabbros from the Llano Uplift, Texas: Petrologic and geochemical characterization with emphasis on tectonic setting: Contrib. Mineral. Petrol. 78:459-475.

Glazner, A. F. 2007. Thermal limitations on incorporation of wall rock into magma. Geol. 35 (4):319-322.

IAG (International Association of Geoanalysts). 2015. Reference Material Data Sheet: SdAR-M2 Metal-rich sediment. https://iageo.com/wp-content/uploads/2019/06/SdAR-M2-RM-information-sheet3-revision-2r.pdf. (Accessed: May 12, 2023).

Levine, J. S. F. & S. Mosher. 2010. Contrasting Grenville-aged tectonic histories across the Llano Uplift, Texas: New evidence for deep-seated high-temperature deformation in the western uplift. Lithosphere 2(6):399-410.

Mosher, S., A. M. Hoh, J. A. Zumbro & J. F. Reese. 2004. Tectonic evolution of the eastern Llano uplift, central Texas: A record of Grenville orogenesis along the southern Laurentian margin. Pp 783-798, *in* Proterozoic tectonic evolution of the Grenville orogen in North America: Boulder, Colorado, Geological Society of America Memoir (R. P. Tollo, L. Corriveau, J. McLelland & M. J. Bartholomew, eds.,197.

Mosher, S., J. S. F. Levine & W. D. Carlson. 2008. Mesoproterozoic plate tectonics: A collisional model for the Grenville-aged orogenic belt in the Llano uplift, central Texas. Geol. 36(1):55-58.

Nelis, M. K., S. Mosher & W. D. Carlson. 1989. Grenville-age orogeny in the Llano Uplift of central Texas: Deformation and metamorphism of the Rough Ridge Formation. Geol. 101:876-883.

Smith, R. K., Gray, W., Gibbs, T. & M. A. Gallegos. 2010. Petrogenesis of Mesoproterozoic granitic plutons, eastern Llano Uplift, central Texas, USA. Lithos. 118:238-254.

Tibbits, T. L. B., Peuramaki-Brown, M. M., Burg, M. B., Tibbits, M. A. & E. Harrison-Buck. 2022. Using X-ray fluorescence to examine ancient Maya granite ground stone in Belize. Geoarchaeology. 28:156-173.

USGS (United States Geological Survey). 2014. Pocket Texas Geology. https://txpub.usgs.gov/txgeology/. (Accessed: June 1, 2022).

Young, K. E., Evans, C. A., Hodges, K. V., Bleacher, J. E. & T. G. Graff. 2016. A review of the handheld X-ray fluorescence spectrometer as a tool for field geologic investigations on Earth and in planetary surface exploration. Appl. Geochem. 72:77-87.